Stem Cells and Regenerative Medicine

The reciprocal regulation between mitochondrial-associated membranes and Notch signaling in skeletal muscle atrophy

Reviewed Preprint

Revised by authors after peer review.

About eLife's process

Reviewed preprint version 2
December 7, 2023 (this version)

Reviewed preprint version 1
August 25, 2023

Posted to bioRxiv
July 20, 2023

Sent for peer review
June 20, 2023

Yurika Ito, Mari Yamagata, Takuya Yamamoto, Katsuya Hirasaka, Takeshi Nikawa, Takahiko Sato

Faculty of Medical Sciences, Fujita Health University, Toyoake, Japan • Department of Biomedical Engineering, Faculty of Life and Medical Sciences, Doshisha University, Kyotanabe, Japan • Center for iPS Cell Research and Application, Kyoto University, Kyoto, Japan • Organization for Marine Science and Technology, Nagasaki University Graduate School, Nagasaki, Japan • Department of Nutritional Physiology, Institute of Medical Nutrition, Tokushima University Graduate School, 3-18-15 Kuramoto-cho, Tokushima, Japan • Department of Ophthalmology, Kyoto Prefectural University of Medicine, Kyoto, Japan • Department of Anatomy, Faculty of Medicine, Fujita Health University, Toyoake, Japan • International Center for Cell and Gene Therapy, Fujita Health University, Toyoake, Japan

Abstract

Skeletal muscle atrophy and the inhibition of muscle regeneration are known to occur as a natural consequence of aging, yet the underlying mechanisms that lead to these processes in atrophic myofibers remain largely unclear. Our research has revealed that the maintenance of proper mitochondrial-associated endoplasmic reticulum membranes (MAM) is vital for preventing skeletal muscle atrophy in microgravity environments. We discovered that the deletion of the mitochondrial fusion protein Mitofusin2 (MFN2), which serves as a tether for MAM, in human iPS cells or the reduction of MAM in differentiated myotubes caused by microgravity interfered with myogenic differentiation process and an increased susceptibility to muscle atrophy, as well as the activation of the Notch signaling pathway. The atrophic phenotype of differentiated myotubes in microgravity and the regenerative capacity of Mfn2-deficient muscle stem cells in dystrophic mice were both ameliorated by treatment with the gamma-secretase inhibitor DAPT. Our findings demonstrate how the orchestration of mitochondrial morphology in differentiated myotubes and regenerating muscle stem cells plays a crucial role in regulating Notch signaling through the interaction of MAM.

Plain-language summary

This study investigated the link between Mfn2 and Notch signaling in skeletal muscle atrophy. We used a microgravity system to induce muscle atrophy and found that the loss of Mfn2 leads to decreased numbers of MAM and activation of Notch signaling and that treating MFN2-deficient human iPS cells with a gamma-secretase inhibitor DAPT improved their mitochondrial morphology and function. Additionally, Mfn2-deficient muscle stem cells in mice have a lower capacity to regenerate dystrophic muscles and DAPT treatment improves the regeneration of these cells. The study suggests that targeting the Notch signaling pathway

with a gamma-secretase inhibitor could be a therapeutic option for skeletal muscle atrophy caused by defects in Mfn2.

eLife assessment

This interesting and **important** manuscript combines in vitro and in vivo experiments to investigate the reciprocal regulation between mitochondria-associated membranes and Notch signaling in skeletal muscle atrophy, with implications beyond the single subfield of muscle atrophy. The methods, data, and analyses are **solid** and broadly support the claims.

Introduction

Skeletal muscles play a vital role in body posture, movement and in regulating metabolism. Regular physical activity helps to maintain muscle mass, while decreased use of skeletal muscle can lead to muscle atrophy (*Bodine et al., 2001*; *Sandri et al., 2004*). This can occur in a variety of disease states, such as muscular dystrophies, as well as in conditions where movement is limited, such as long-term bed rest or injury-induced immobility, or even in microgravity conditions during spaceflight (*Gao et al., 2018*). Additionally, muscle loss is a common aspect of the aging process (*Larsson et al., 2017*; *Distefano and Goodpaster, 2018*). The mechanisms of disuse-induced muscle atrophy and the impact on regenerative capacity in skeletal muscle have been extensively studied in various animal models, including humans.

Mitochondria are essential for maintaining tissue homeostasis and supplying adenosine triphosphate (ATP) during muscle development and regeneration. This is particularly important in energy-intensive myogenic cells, such as differentiated myofibers and muscle stem cells, as they mature (*Duguez et al., 2002*; *Ryall 2013*; *Bhattacharya et al., 2020*). The shape and size of mitochondria in mature myofibers undergo drastic changes to meet the energy demands of developmental growth, the switch between slow- and fast-twitch myofibers, exercise, and aging (*Ljubicic et al, 2010*; *Wyckelsma et al., 2017*). These morphological and functional changes in mitochondria are facilitated by the processes of fission and fusion, respectively (*Youle and van der Bliek, 2012*). Mitochondrial fusion is regulated by the transmembrane GTPase proteins, Mitofusin1 (Mfn1) and Mitofusin2 (Mfn2), which are located on the outer mitochondrial membrane (*Chen et al., 2003; Eura et al., 2003*; *Sin et al., 2016; Youle and van der Bliek, 2012*).

Ablation of both Mfn1 and Mfn2 leads to embryonic lethality in mice, while muscle-specific inactivation of *Mfn1* and *Mfn2* genes results in severe mitochondrial dysfunction and muscle atrophy (*Chen et al., 2003*; *Chen et al., 2010*). Mfn2, in particular, is necessary to tether the endoplasmic reticulum (ER) to mitochondria, thereby enhancing mitochondrial energetics (*de Brito and Scorrano, 2008; Filadi et al., 2018*; *Ishihara et al., 2004*). However, the specific role of the mitochondria-ER complex in developmental, regenerative, and atrophic processes in skeletal muscle remains unclear. Our research has revealed that muscle atrophy is linked to Mfn2 and the Notch signaling pathway, as demonstrated by the use of MFN2 knockout human induced pluripotent stem (iPS) cells, primary human myoblasts, and mice.

Our research demonstrates that the restoration of ER-mitochondria contacts through the regulation of Notch signaling is sufficient to partially alleviate the bioenergetic defects in MFN2-deficient human iPS cells or myogenic cells. This suggests that treatment with gamma-secretase

inhibitors may be a viable therapeutic option in pathological conditions in which Mfn2 is involved. These findings provide new insights into the treatment of skeletal muscle atrophy caused by mitochondrial abnormalities.

Results

Human primary myotubes exhibit an atrophic phenotype in a microgravity environment

To investigate the effects of microgravity on skeletal muscle atrophy, we utilized a 3D-clinorotation system to simulate microgravity conditions with human primary skeletal muscle hOM2 cells, which are derived from the orbicularis oculi (*Yamanaka et al., 2019*). We observed that the proliferation of both myogenic cells and human iPS cells decreased in microgravity using the clinorotation (*Supplementary file 1*), and it has been reported that initial myogenic differentiation to form myotubes is suppressed by fluid motion when the clinorotation is used (*Mansour et al., 2023*). Therefore, we examined differentiated myotubes derived from primary hOM2 cells after confluence, both with and without the clinorotation (***Figure 1A***). These primary cells were mainly differentiated into *MYH7*-positive type 1 slow-twitch myotubes after 7 days (*Supplementary file 2*), and we found that these differentiated myotubes in microgravity, when cultured for 7 days, were more fragile and tenuous in appearance than those cultured for 2 days, compared to controls (the bottom images in ***Figure 1B***). We also observed an increase in the transcripts of *MuRF1* and *FBXO32* (*Atrogen1/MAFbx*), which are markers of muscle atrophy, in these myotubes, as the duration of microgravity increased (***Figure 1C*** *and* ***1D****)*. However, the expression of *MRF4* and *MYH3*, early myogenic differentiation markers, and Caspase-3 and phospho-AKT, apoptotic markers, were not altered (***Figure 1C*** and *Supplementary file 3*). To investigate the condition of MAM in differentiated myotubes, we utilized a proximity ligation assay (PLA) with antibodies against the voltage-dependent anion channel 1 (VDAC1) of mitochondria and the inositol 1,4,5-triphosphate receptor (IP3 receptor) of the ER (*Prole and Taylor, 2019; Shoshan-Barmatz et al., 1996*). Previous studies have demonstrated that PLA can occur within a range of 40nm, which aligns with findings suggesting that optical Ca^{2+} transfer necessitates a mitochondrial proximity of approximately 20nm (*Gottschalk et al., 2022; Lim et al., 2021*). We found that the number of MAM was severely decreased in microgravity, specifically in differentiated multinucleate myotubes rather than undifferentiated myoblasts (***Figure 1E*** *and* ***1F***). It has been previously reported that the mitochondrial fusion protein MFN2 tethers MAM. We found that the protein level of MFN2 was decreased in differentiated myotubes under microgravity conditions, although the mRNA level was not significantly changed (*Supplementary file 4*).

Mitochondrial abnormality in human MFN2-deficient iPS cells

To investigate the role of MFN2 in atrophic myotubes differentiated from human iPS cells, we generated MFN2-mutated human iPS cells by introducing a double-strand break in the MFN2 exon3, which includes the coding sequence, using the pX458-hMFN2 editing vector with guide RNA, and two different knock-in oligos (ssODN, *Supplementary file 5A and 5B*). The electroporated cells were plated on SNL feeder cells, and single cells exhibiting GFP expression were sorted through bicistronic expression with guide RNA, expanded, and subsequently, the genomic DNA was screened for the correct insertion of the knock-in reporter cassette. The genomic sequencing showed that the selected clone contained the oligo cassette (*Supplementary file 5B*). This clone was confirmed to retain the pluripotency of undifferentiated human iPS cells using antibodies against NANOG or TRA1-81, however, the expression of MFN2 was not detected using an antibody against MFN2 (*Supplementary file 5C and 5D*).

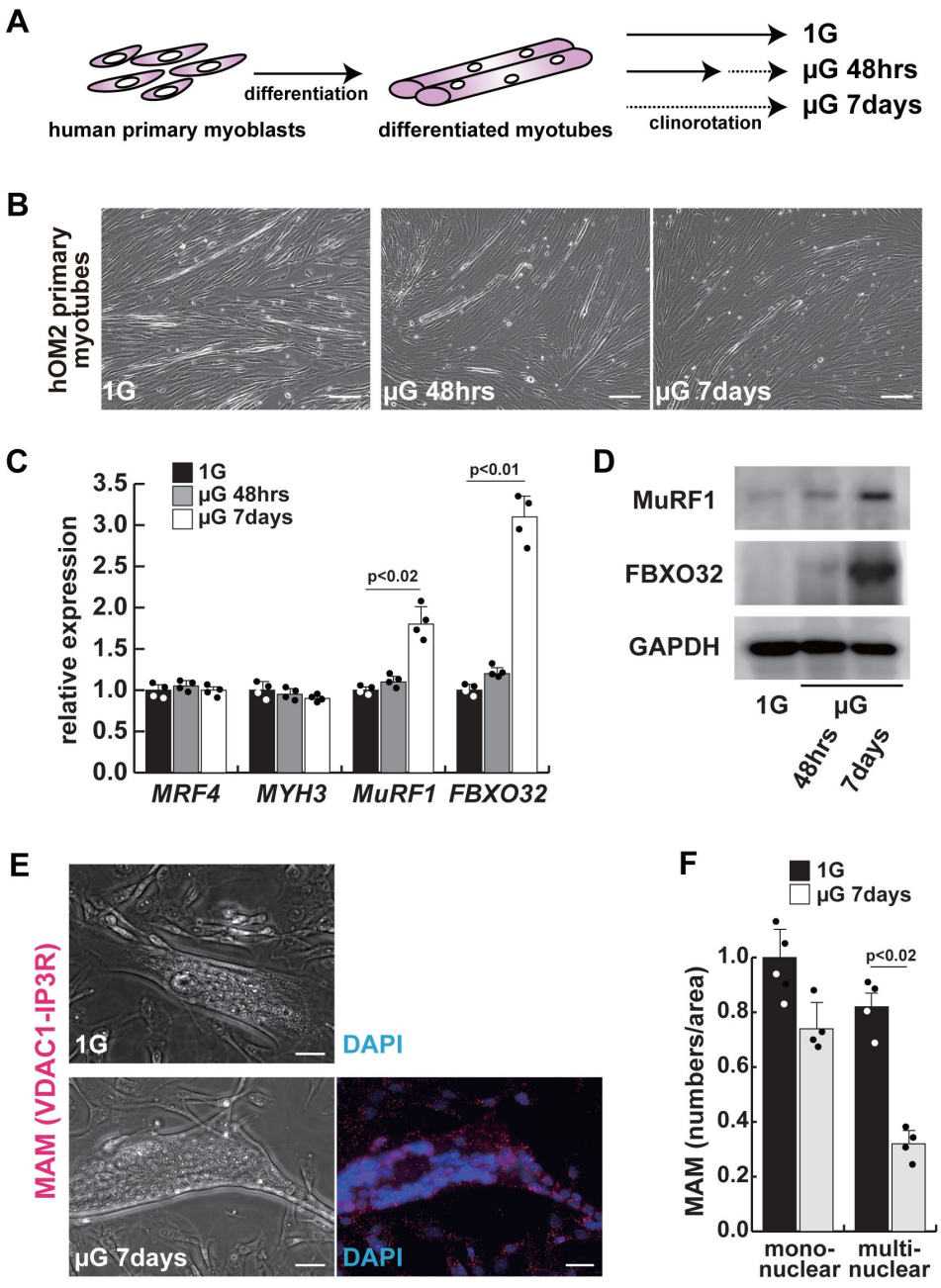

Figure 1.

The integrity of the mitochondrial-associated ER membrane is compromised by microgravity in differentiated primary human myotubes. (A) A diagrammatic representation of differentiated human myotubes under normal conditions or exposed to clinorotation. μG; microgravity. (B) Phase contrast images of differentiated primary human myotubes under 1G (upper panel) and μG for 48 hours (left lower panel), for 7 days (right lower panel). Scale bars; 50 μm. (C) Transcription levels of *MRF4* (myogenic determination), *MYH3* (early differentiation), *MuRF1* and *FBXO32* (muscle atrophy) in differentiated myotubes with or without microgravity, measured by RT-qPCR and presented relative to transcripts of ribosomal protein RPL13a. (D) Western Blotting analyses of lysates from differentiated myotubes with or without microgravity. Nuclear lysates were analyzed with antibodies against MuRF1 and FBXO32. GAPDH was used as a loading control. (E) Phase contrast images and detectable adjacent mitochondria-associated ER membranes (MAM) by Proximal Ligation Assay in differentiated myotube. Scale bars; 20 μm. (F) The number of MAM in mononuclear myoblasts (mononuclear) or multinucleated fused myotubes (multinuclear) per fixed area. All error bars indicate ±SEM (n=4). *P*-values are determined by non-parametric Wilcoxon tests or one-way ANOVA and Tukey's test for comparisons.

We further examined the mitochondrial condition using MFN2-deficient human iPS cells. MFN2-deficient human iPS cells showed a decrease in the number of MAM, similar to that observed in differentiated myotubes under microgravity (***Figure 2A*** *and* ***2B***). Additionally, these cells exhibited abnormalities in mitochondrial fission (***Figure 2C***) (*Cartoni et al., 2009; Ohara et al., 2017*) and a decrease in ATP production (***Figure 2D***). To investigate the effect of MFN2 in human iPS cells, we performed next-generation sequencing (NGS) analyses comparing normal MFN2 (201B7, PB-MYOD) (*Takahashi et al., 2007; Tanaka et al., 2013*) to deficient MFN2 ($MFN2^{-/-}$) human iPS cells (*Supplementary file* 6). We found that among the upregulated mRNAs expressed in MFN2-deficient iPS cells, the expression levels of Notch-related factors, such as genes of the HES or ID family, were significantly higher as shown by NGS and RT-qPCR analyses (*Supplementary file 6 and 7*). In keeping with these findings, we observed that MFN2-deficient human iPS cells activated the Notch intercellular domain (NICD) in nuclei (red in ***Figure 2E***). The expression levels of these upregulated factors related to Notch signaling in the MFN2-knockout condition were further increased in the microgravity condition (***Figure 2F***). To investigate the effects of MFN2 deficiency on differentiated myotubes derived from human iPS cells, these cells were induced by MYOD, activated by Doxycycline (*Sato et al., 2019*), cultured *in vitro* under differentiation conditions, and immunostained for MYHC expression as an indicator of their ability to differentiate into myotubes. We found that the number of differentiated myotubes derived from MFN2-deficient human iPS cells was significantly lower than that of wildtype cells (*Supplementary file 8A and 8B*). The activation of Notch signaling was also consistent with its increase in MFN2-deficient human iPS cells (*Supplementary file 8C*). These data indicate that the formation of differentiated myotubes derived from human iPS cells compromised in the absence of MFN2.

The rescue of mitochondrial defects in human MFN2-deficient iPS cells by gamma-secretase inhibitor

We have confirmed that MFN2-deficient iPS cells showed abnormal mitochondrial morphology, MAM, and function. In these MFN2-deficient cells, Notch signaling was activated as recently reported in cardiomyocytes, where it was shown that the elevated Notch signaling in MFN2-deficient conditions was caused by the enzymatic activation of Calcineurin (*Kasahara et al., 2013*). We observed upregulation of Calcineurin activity in human iPS cells in the absence of MFN2 and in primary human muscle cells under microgravity (*Supplementary file* 9). We therefore investigated whether the inhibition of upregulated Notch or Calcineurin pathways could ameliorate mitochondrial functions in MFN2-deficiency. MFN2-deficient hiPS cells were treated with a gamma-secretase inhibitor, DAPT, and the inhibitor of Calcineurin activity, FK506. We found that DAPT, but not FK506, improved mitochondrial morphology in these cells (***Figure 3A*** and *Supplementary file* 10). MFN2-deficient hiPS cells, treated with DAPT, showed decreased expression of activated HES family genes such as *HES1* and *HEY1* (***Figure 3B***). We found that the number of MAM in these cells treated with DAPT, was increased (***Figure 3C*** *and* ***3D***). Additionally, when DAPT was administrated to MFN2-deficient hiPS cells, we observed an increase in total ATP production (***Figure 3E***). These results suggest that mitochondrial functions depending on MAM, are closely linked to Notch signaling.

Gamma-secretase inhibitor DAPT ameliorates the atrophic phenotype in differentiated human myotubes under microgravity

To investigate the effect of microgravity on Notch signaling in differentiated myotubes, we evaluated Notch expression in primary human muscle cell cultures. We found that among Notch receptors, expression of the Notch2 transcript was highest in growing myoblasts and differentiated myotubes (*Supplementary file 11*). We confirmed the activation of the Notch2-intercellular domain in both differentiated myotubes derived from MFN2-deficient human iPS cells (***Figure 4A***) and in primary differentiated myotubes, exposed to microgravity (***Figure 4B***

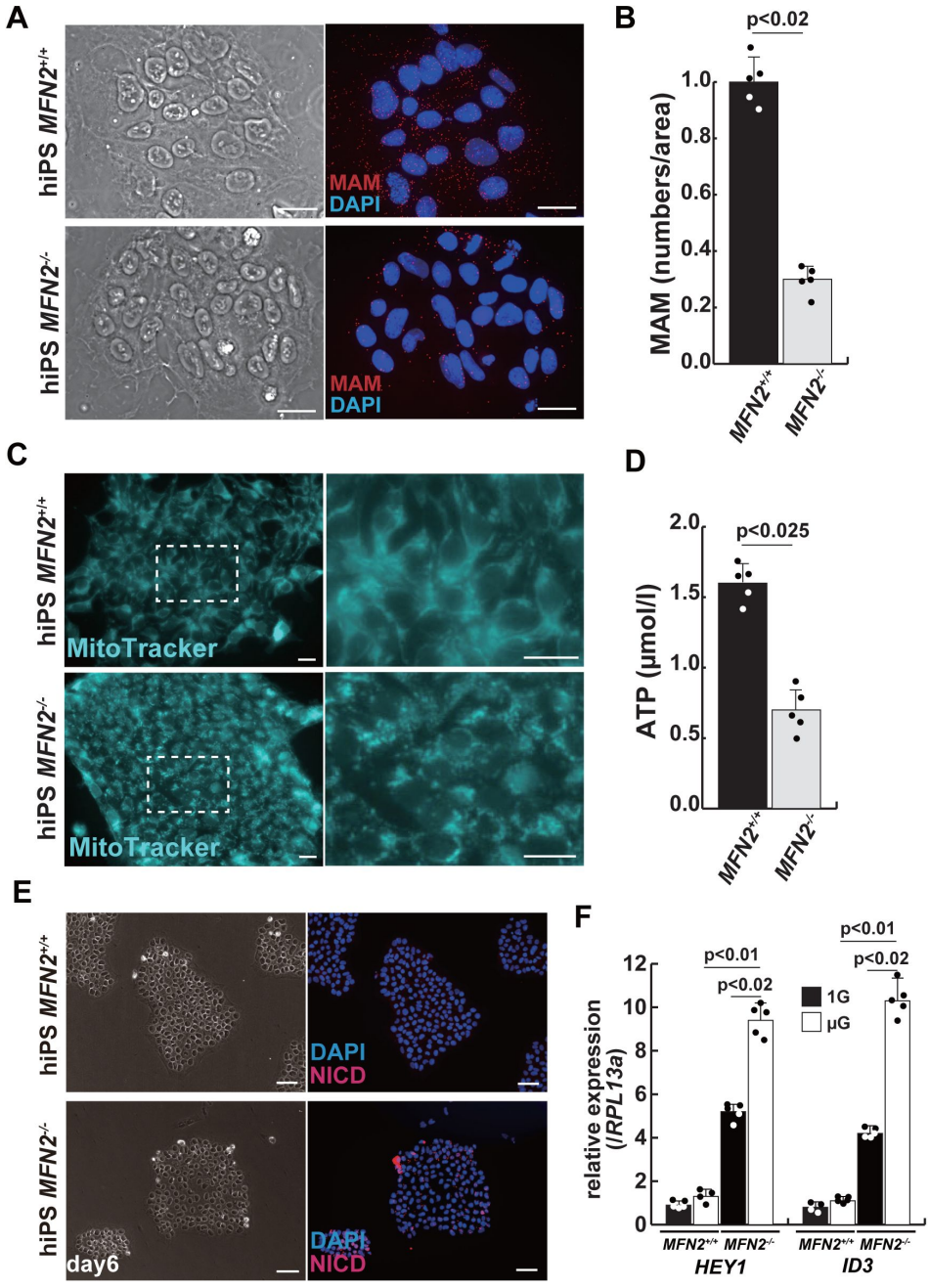

Figure 2.

Mitochondrial abnormality and the activation of Notch in MFN2-deficient human iPS cells. (A) Phase contrast images (left panels) and MAM visualization (right panels) with or without MFN2 in human iPS cells. Red; MAM (IP_3R-VDAC1 by PLA), blue; DAPI, Scale bars; 20 μm. (B) The quantitative analyses of MAM numbers per fixed area in human iPS cells with or without MFN2. (C) Mitochondrial morphology with MitoTracker in human iPS cells with or without MFN2. (Right panels; magnified area outlined in each left panel), Scale bars; 50 μm. (D) Total ATP production (μmol/l) in wild-type or MFN2-deficient human iPS cells. (E) Phase contrast (left images) and Immunostaining for Notch-intercellular domain (NICD; Red) and DAPI (blue) on wild-type or MFN2-deficient human iPS cells (right images). Scale bars; 50 μm. (F) Relative transcription levels of *HEY1* and *ID3* in wild-type or MFN2-deficient human iPS cells under normal gravity (1G) or microgravity (μG). All error bars indicate ±SEM (n=5). *P*-values are determined by non-parametric Wilcoxon tests for comparisons.

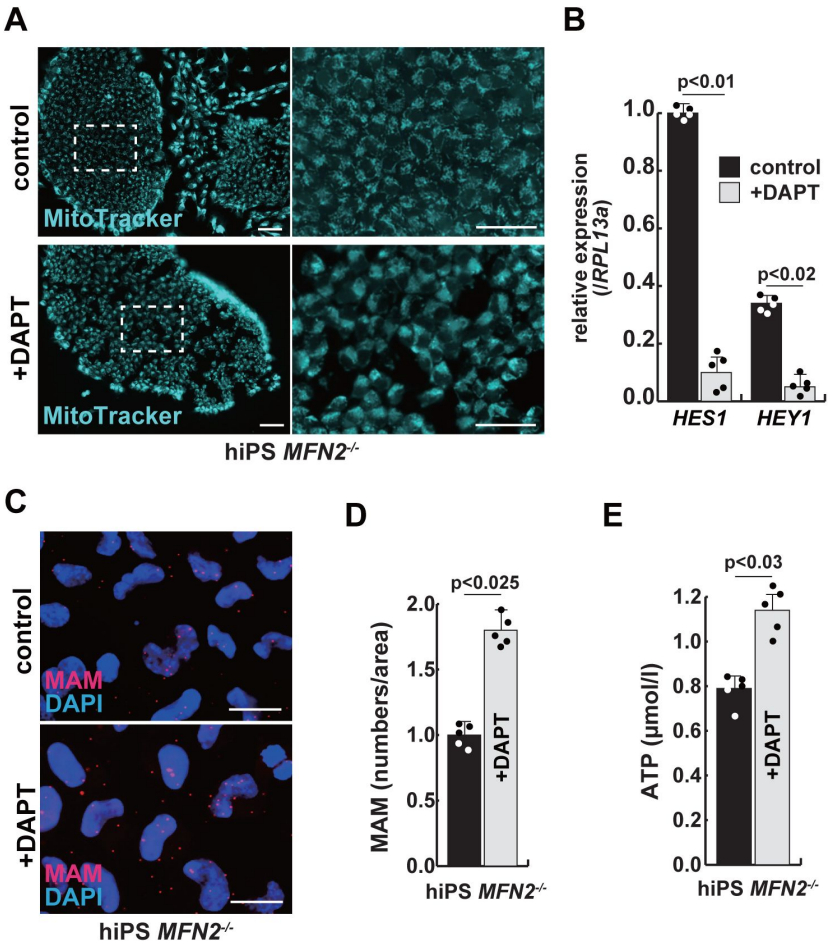

Figure 3.

The improvement of mitochondrial abnormalities in MFN2-deficient human iPS cells treated with gamma-secretase inhibitor DAPT. (A) Mitochondrial morphology visualized by MitoTracker in MFN2-deficient human iPS cells with or without 50μM of DAPT. (Right panels; magnified area outlined in right panels), Scale bars; 50 μm. (B) Relative transcription levels of *HES1* and *HEY1* in MFN2-deficient human iPS cells with or without DAPT. (C) MAM visualization in MFN2-deficient human iPS cells, with or without DAPT. (Red; MAM (IP3R-VDAC1 PLA), blue; DAPI, Scale bars; 20 μm. (D) The quantitative analyses of MAM numbers in MFN2-deficient human iPS cells with or without DAPT. (E) Total ATP production in MFN2-deficient human iPS cells treated with or without DAPT. All error bars indicate ±SEM (n=5). *P*-values are determined by non-parametric Wilcoxon tests for comparisons.

with arrowheads). The latter also showed upregulation of Notch-related genes such as members of the HES family or ID family (***Figure 4C***) and a decline in ATP production in these cells under microgravity (***Figure 4D***).

To test the effect of inhibition of Notch signaling on the diminished mitochondrial function and increased expression of atrophic markers seen under microgravity, we administered DAPT every 2 days to cultured myotubes under microgravity (***Figure 4E***). After treatment with DAPT, we observed a significant decrease in the expression of HES family genes such as *HES1* and *HEY1* (***Figure 4F***), positive changes in mitochondrial morphology (***Figure 4G***), and partial recovery of the numbers of MAM (***Figure 4H***). Additionally, we observed an increase in total ATP production (***Figure 4I***). These results indicate that gamma-secretase inhibitors are effective in improving the mitochondrial phenotype, not only in MFN2-deficient hiPS cells but also in differentiated myotubes induced by microgravity. We also found that the treatment with DAPT, led to a reduction in the level of atrophic markers such as *MuRF1* or *FBXO32* (***Figure 4J***), and a partial restoration of *MYH7* expression (*Supplementary file 12*). These results suggest that elevated Notch signaling is casual in these adverse effects,

Muscle stem cells derived from conditional *Mfn2* mutant mice show decreased MAM and higher Notch activity, with reduced regenerative capacity of these mice after repeated injury

To further investigate the effect of Mfn2 deficiency on skeletal muscle stem cells (satellite cells) *in vivo*, we generated conditional Mfn2-knockout mice ($Mfn2^{loxP/loxP}$; $Pax7^{CreERT2/+}$), carrying an inducible Pax7-CreERT2 allele that targets muscle stem cells (***Figure 5A***). Isolated SM-C/2.6-positive muscle stem cells from these mice were treated with Tamoxifen to induce Mfn2 deficiency, and then co-cultured with non-myogenic fibroblasts, as a control for muscle-specific mutation of *Mfn2* with differentiation into myotubes. We found that Mfn2 staining was present in non-myogenic fibroblasts and myotubes derived from control mice, but not in myotubes derived from Mfn2-deficient muscle stem cells (arrowheads in ***Figure 5B***) As expected, the expression of Mfn2 was faint in muscle stem cells, and gradually increased in differentiated muscle fibers (*Luo et al., 2021*). Additionally, the number of MAM was decreased in differentiated myotubes derived from Mfn2-deficient muscle stem cells, as previously seen in MFN2-deficient human iPS cells or cultured myotubes under microgravity (***Figure 5C***). Furthermore, increased nuclear NICD protein was observed in cultured Mfn2-deficient muscle stem cells (***Figure 5D***). The stemness characteristics of Mfn2-deficient muscle stem cells, as indicated by Pax7 expression, were not significantly altered. However, the proportion of elongated myogenic cells in cultures of Mfn2-deficient muscle stem cells was impeded (*Supplementary file 13*).

Next, we induced muscle injury by injecting cardiotoxin (CTX) into the tibialis anterior (TA) muscle of these conditional Mfn2-knockout mice after 4-OH tamoxifen treatment *in vivo* to prevent *Mfn2* expression specifically in muscle stem cells. The TA muscle of control mice was similarly injured and muscle regeneration was examined. We found that while there was no significant difference in muscle regeneration between the two groups 2 weeks after CTX injection (*Supplementary file 14*), Mfn2-deficient mice showed a reduced capacity for muscle regeneration after repeated injury. Additionally, the regenerated muscle in Mfn2-deficient mice did not exhibit the normal hypertrophic phenotype seen in control mice. (*Supplementary file 15*) (*Hardy et al., 2016*). These results suggested that Mfn2 deficiency diminishes the regenerative capacity of muscle stem cells in chronic degenerative contexts.

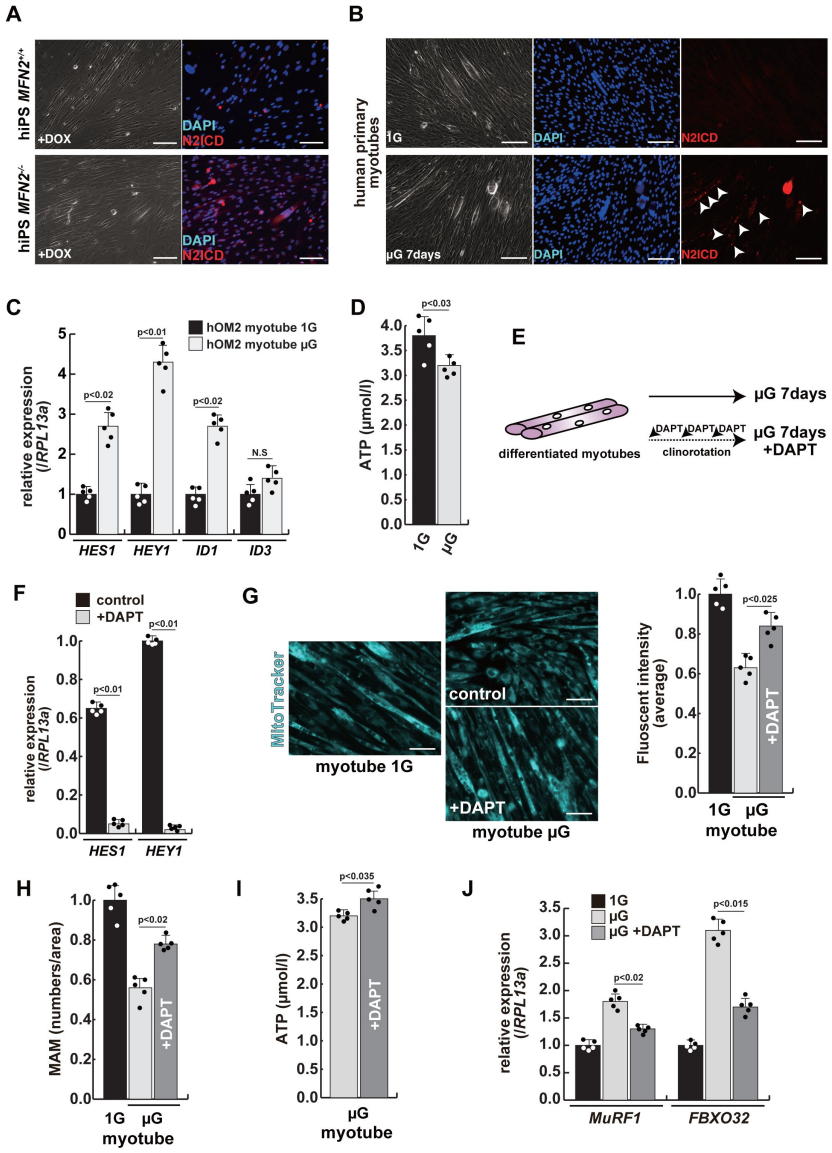

Figure 4.

The atrophic phenotype of human myotubes under microgravity is alleviated by the gamma-secretase inhibitor DAPT. (A) Phase contrast (left panels) and Immunostaining (right panels) for NOTCH2-intercellular domain (N2ICD; Red) and DAPI (blue) on differentiated myotubes derived from wild-type, or MFN2-deficient human iPS cells by Doxycycline (DOX) treatment. Scale bar; 50 μm. (B) Phase contrast images (left panels) and immunostaining for NOTCH2-intercellular domain (right panels, N2ICD; Red) and DAPI (middle panels, blue) on differentiated myotubes under normal gravity (1G) or microgravity (μG) for 7 days. Scale bar; 50 μm. (C) Relative transcription levels of HES family genes *(HES1, HEY1)* and ID family genes (*ID1*, *ID3*) in differentiated myotubes derived from wild-type or MFN2-deficient human iPS cells after Doxycycline (DOX) treatment. (D) Total ATP production in differentiated human primary myotube under normal gravity (1G) or microgravity (μG) for 7 days. (E) The schematic representation of differentiated human primary myotubes under microgravity (μG) for 7 days with or without DAPT. (F) Relative transcription levels of *HES1* or *HEY1* in differentiated human primary myotubes under microgravity for 7 days with or without DAPT. (G) Mitochondrial morphology with MitoTracker in differentiated human primary myotubes under normal gravity (1G; left panel) and microgravity with or without DAPT (μG; upper and lower left panels). The average fluorescent intensity of total cells treated with MitoTracker is indicated on the right. Scale bars; 50 μm. (H) Quantitative analyses of MAM numbers in differentiated human myotubes under microgravity with or without DAPT. Scale bar; 50 μm. (I) Total ATP production in differentiated human myotubes under microgravity with or without DAPT. (J) Relative transcription levels of *MuRF1 and FBXO32* (muscle atrophy) in differentiated human primary myotubes under normal gravity (1G) and microgravity (μG) with or without DAPT for 7 days. All error bars indicate ±SEM (n=5). *P*-values are determined by non-parametric Wilcoxon tests or one-way ANOVA and Tukey's test for comparisons. N.S; not significant.

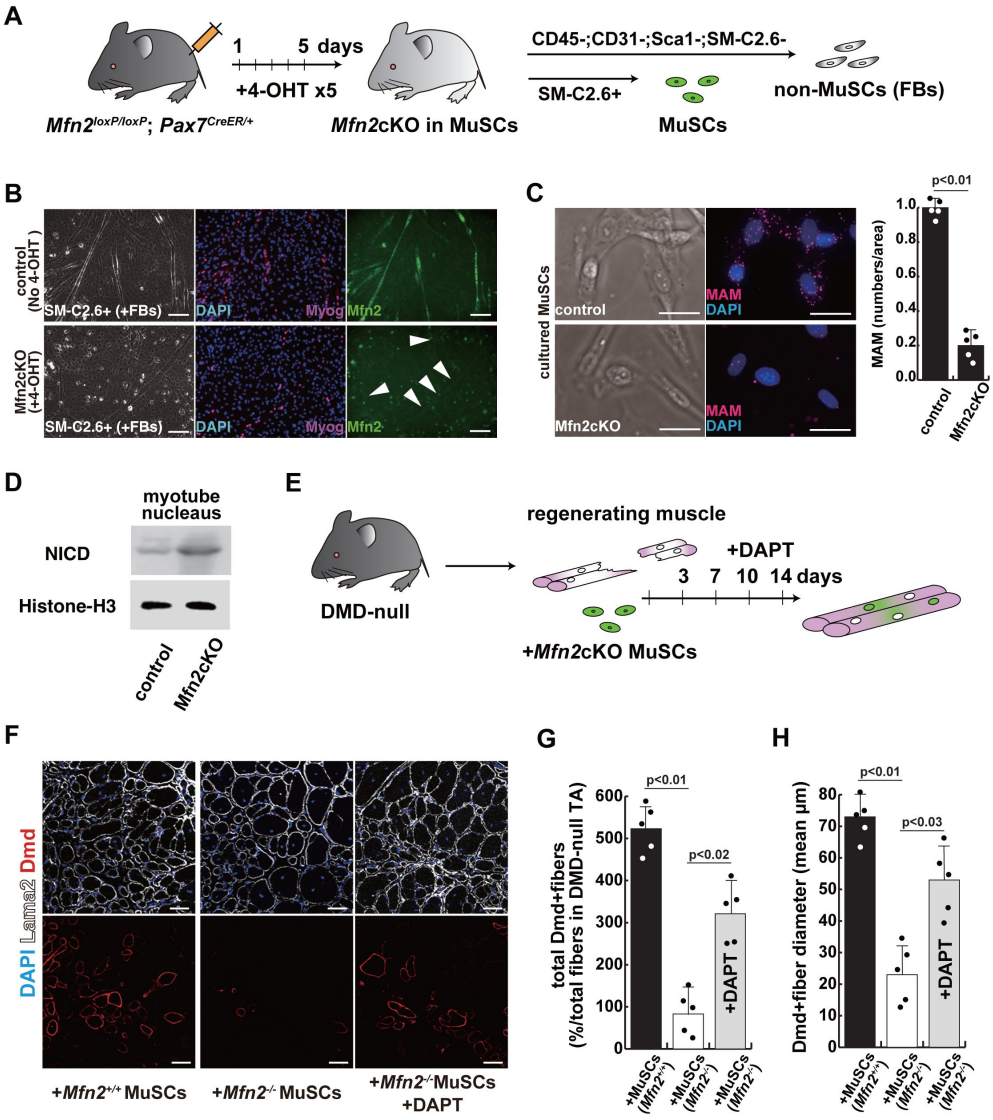

Figure 5.

The regenerative capacity of Mfn2-deficient mouse muscle is reduced and that of Mfn2-deficient muscle stem cells when transplanted into Dystrophic muscle in vivo is improved by DAPT treatment of the muscle. (A) The flowchart to isolate muscle stem cells (MuSCs, SM-C/2.6+) and non-myogenic fibroblasts (FBs) derived from conditionally Mfn2 knockout mice after 4-OH tamoxifen (4-OHT) injection. (B) Immunostaining for Mfn2 (Green), Myogenin (Myog; Red), and DAPI (blue) on differentiated myotubes derived from wildtype or Mfn2-deficient mouse muscle stem cells sorted as SM-C/2.6 positive cells, co-cultured with non-myogenic fibroblasts (FBs). Scale bar; 50 μm. (C) Phase contrast images (left panels) and MAMs visualization (right panels) and quantitative analyses of MAM numbers (right) on cultured muscle stem cells. (Red; MAM (IP3R-VDAC1 PLA), blue; DAPI, Scale bars; 20 μm. (D) Western Blotting analyses of lysates from control and Mfn2-mutant cultured muscle stem cells. Nuclear lysates were analyzed with antibodies against NICD. Histone H3 was used as a loading control. (E) The flowchart for the transplantation into tibialis anterior (TA) muscles of *DMD*$^{-/y}$ mice (12 weeks old) with Mfn2-deficient muscle stem cells (1.0 x 10^4 cells) and the treatment with DAPT every 3~4 days after the transplantation. (F) Transverse sectional images of TA muscles 14 days after the transplantation with the same number of muscle stem cells sorted as SM/C-2.6-positive cells derived from wildtype or conditional Mfn2 Knockout mice. Immunostaining for Dystrophin (Dmd, red as transplanted areas), laminin-a2 (Lama2, white to show the outline of myofibers), and DAPI (blue) on engrafted TA muscle after the transplantation. Scale bars; 50 μm. (G) The quantification of the total number of Dystrophin-positive (Dmd+) regenerated myofibers on the section transplanted with an equivalent number of normal or Mfn2-deficient MuSCs, with or without the treatment of the transplanted muscle with DAPT. (H) The average diameter of Dystrophin-positive (Dmd+) myofibers that are contributed by the transplanted MuSCs, as described in (G). All error bars indicate ±SEM (n=5). *P*-values are determined by non-parametric Wilcoxon tests or one-way ANOVA and Tukey's test for comparisons.

The regenerative capacity of transplanted Mfn2-deficient muscle stem cells is improved by inhibition of the Notch pathway

As a model to test regeneration after cell transplantation, we used dystrophic muscle which represents a chronic degenerative context. We transplanted SM-C/2.6-positive muscle stem cells, from wildtype, or conditional Mfn2 knockout mice after 4-OH tamoxifen treatment, into the TA muscle of *Dmd*$^{-/y}$dystrophic mice, with or without DAPT treatment (***Figure 5E***). Our findings indicated that Mfn2-deficient muscle stem cells were less capable of integrating into dystrophic muscles, as evidenced by decreased Dystrophin expression (middle panel in ***Figure 5F***). However, notably, DAPT treatment of the TA muscles post-transplantation in this context led to increased Dystrophin expression and a larger size of regenerated myofibers (lower panel in ***Figure 5F-H***).

Discussion

Skeletal muscle atrophy is caused by various factors, including disuse or mechanical unloading. Here we found that diminished MAM, mitochondrial-associated ER-membrane, is associated with muscle atrophy in the microgravity condition. The result of our studies demonstrated the essential role of MAM in the regulation of skeletal muscle atrophy. MAM is considered to serve as a Ca^{2+} transit point from the ER to mitochondria and is regulated not only by MFN2 but by the IP3R-VDAC1 protein complex (*Rizzuto et al., 1998*) which releases Ca^{2+} from the ER and participates in its transfer to the mitochondria (*Szabadkai et al., 2006*). We have therefore measured the proximity of these protein complexes by the PLA method, as reported in liver, or kidney cells (*Alam, 2018; D'Eletto et al., 2018; Theurey et al., 2016*).

Mfn2 is a key factor in regulating mitochondrial fusion, which is affected by the GTPase activity of both Mfn1 and Mfn2 on the mitochondrial outer membrane. It has been reported that Mfn2 but not Mfn1 independently regulates not only MAM, but also mitophagy, obesity, cardiomyopathies, and several neuronal defects such as Charcot-Marie-Tooth disease, and Parkinson's disease, suggesting that Mfn2 might not functionally compensate for Mfn1 (*Chen and Dorn, 2013; Filadi et al., 2018; Sebastián et al., 2016*). Our experiments with MFN2-disrupted iPS cells, also indicated that the numbers of MAM were decreased and affected mitochondrial functions. However, no effect on developmental myogenesis or growth was observed in Mfn2-deficient mice, which showed comparable to that of wild-type mice. In muscle regeneration, Mfn2-deficient mice showed little change from wild-type mice in the event of a single muscle injury. In contrast, Mfn2 deficiency caused a muscle atrophy-like phenotype in vitro culture, however, no such muscle atrophy is observed with muscle-specific Mfn2 deficiency in vivo (*Luo et al., 2021*). One potential explanation for this discrepancy is that cell culture conditions introduce excessive mechanical stress (*Banfanti et al., 2022; Valon and Levayer, 2019*). Indeed *in vivo*, repeated injury of muscle lacking Mfn2 did result in impaired regeneration. Future studies should consider how Mfn2 is involved in adaptation to mechanical stress.

In addition, enhanced Notch signaling was observed accompanying the decrease of MAM in MFN2-deficient iPS cells and myocytes. Reports on cardiac muscle cells suggest that there is crosstalk between Ca^{2+}/calcineurin with MAM and Notch signaling pathways, which may function in addition to, or in parallel with, Notch1 regulation by extracellular calcium and sarcoplasmic reticulum Ca^{2+} adenosine triphosphatase (SERCA) (*Rand et al., 2000; Roti et al., 2013; Song et al., 2022*). Indeed, we report that when human iPS cells in the absence of MFN2 were treated with inhibitors of calcineurin and Notch signaling, the mitochondrial distribution was not significantly altered by FK506, a calcineurin inhibitor, but by DAPT, a Notch signaling inhibitor (*Supplementary file 10*). The same results were obtained in skeletal muscle cells, where changes in mitochondrial distribution were observed and partial functional recovery was demonstrated upon suppression

of Notch signaling. Further research will be necessary to unravel the underlying mechanisms that lead to enhanced Notch signaling in MFN2 deficiency, to explore upstream pathways, other than calcium, and to elucidate the reverse control mechanism by which Notch regulates MAMs.

The Notch signaling pathway is an evolutionarily conserved cascade that plays a role in organ development and morphogenesis, stem cell fate, tissue metabolism, and in various diseases (*Andersson et al., 2011*). In skeletal muscles, Notch signaling is regulated throughout multiple stages of development and regeneration. It is essential for maintaining the dormant state and also for self-renewal of muscle stem cells in the adult (*Gioftsidi et al., 2022; Liu et al., 2018*). The positioning of these stem cells on muscle fibers depends on basal lamina assembly controlled by Notch (*Bröhl et al., 2012*), which also acts as an inhibitor of premature differentiation by repressing the expression of MyoD, a myogenic regulatory factor (*Delfini et al., 2000*). However, its role in myogenesis at late-stages or in mature myotubes remains unclear. In studies involving the forced expression of NICD in differentiating muscle cells, Notch signaling has been shown to inhibit their maturation after myocyte fusion, but also to ameliorate the pathophysiology of mature muscle fibers in aged or dystrophic muscle (*Bi et al., 2016*). The differentiated human muscle cell culture used in this experiment reported here do not form fully mature fibers. Therefore the effects of Notch inhibition by DAPT at later stages, using more highly organized culture systems to prompt maturation, require further investigation.

Activated Notch signaling has been reported in dystrophic or atrophic muscles (*Fujimaki et al., 2022; Sakai-Takemura et al., 2020*) and also in other pathological situations such as neuroblastomas (*Ferrari-Toninelli et al., 2010*) or in ischemic stroke where inhibition of Notch signaling with DAPT is beneficial (*Balaganapathy et al., 2018*). Our study has shown that treatment of DAPT can counteract the negative effect of MFN2 deficiency in human iPS cells and myocytes. Furthermore, grafting efficiency of Mfn2 deficient muscle stem cells is improved if the recipient muscle is treated with DAPT. These experiments point to the positive effects of inhibiting Notch in this context. Importantly, reduction in Notch signaling by DAPT addition in muscle cells under microgravity resulted in higher Mfn2 and MAM levels with improved mitochondrial function and reduced atrophy. This opens the possibility that compounds to inhibit Notch signaling may be of therapeutic value in treating pathological muscle wasting. The treatment of various cancers and of Alzheimer's disease, in which the Notch pathway has been implicated, is in progress (*McCaw et al., 2021; You et al., 2023*). Further investigation will be required to find out whether these gamma-secretase inhibitors are also effective against muscle atrophy and muscle diseases.

Materials and methods

Primary Human Myogenic Cell Culture

Human biopsies of the extra eyelid tissue, including orbicularis oculi muscle were minced and subjected to enzymatic dissociation with 0.1% Collagenase Type2 (Worthington) in DMEM (WAKO) at 37°C for 60 min. Dissociated cells from biopsies or sorted cells were plated in DMEM containing 20% FBS and 5 ng/mL of basic FGF (WAKO), coated with Geltrex (GIBCO). Fresh media was added regularly until colonies with spindle-shaped cells were obtained. For primary myogenic cell sorting, expanded cells were detached with Accutase (Nacalai tesque) from cell culture dishes, resuspended with 1% bovine serum albumin (Sigma-Aldrich) in PBS buffer (WAKO), and incubated with the monoclonal anti-human antibodies anti-CD56-PE and anti-CD82-Alexa647 (BioLegend). After 30 minutes incubation on ice, human myoblasts including muscle stem cells, defined as CD56+CD82+, were sorted by flow cytometry using a FACS JAZZ (BD). Isotype control antibodies were PE- and Alexa647-conjugated mouse IgG1 (BioLegend), filtrated with a cell strainer (35μm, BD). Cell suspensions were stained with SYTOX Green Dead Cell Stain (Molecular Probes) to exclude dead cells. These primary human myogenic cells are referred to as hOM2 cells.

These hOM2 myogenic cells were cultured in DMEM containing 20% of FBS and 5ng/ml of basic FGF. After a few days of cell culture at 70–80% of confluency, these cells were differentiated into myotubes in DMEM supplemented with 2% horse serum (GIBCO).

Human iPS cell culture

Human iPS cells (based on #201B7 line) (*Takahashi et al., 2007*) were cultured on 0.1% of Gelatin-coated dishes in Primate ES cell medium (Reprocell) supplemented with 5ng/mL of basic FGF with SNL feeder cells, or iMatrix (Nippi)-coated dishes in StemFit AK02 medium (Ajinomoto) without feeder cells. human iPS cells were passaged as the condition of single cells. The derivation of myogenic cells from hiPS cells based on MYOD1 induction (*Sato et al., 2019; Tanaka et al., 2013*), was followed. Single iPS cells carrying an inducible MYOD1 activation system were expanded in Primate ES cell medium (Reprocell) without bFGF and with 10μM of Y-27632 (Nacalai tesque) for 24 hours, and then induced into myogenic cells by adding 500ng/ml of Doxycycline (DOX; Tocris). After 24 hours, the cell culture medium was changed into myogenic differentiation medium composed of alpha-MEM (Nacalai tesque) with 5% of KSR (GIBCO) and 500ng/ml of Dox. After 6 days, the culture medium was changed into muscle maturation medium, DMEM/F12 with 5% of horse serum, 10ng/ml of recombinant human insulin-like growth factor 1 (IGF-1; Peprotech), and 200μM of 2-Mercaptoethanol (2-ME; Sigma-Aldrich).

hMFN2 targeting with human iPS cells

To introduce into cultured cells with hMFN2-targeting vector by CRISPR/Cas9 system, which was constructed with pX458 vector (Addgene #42230) by ligating oligos into it (MFN2 exon3 target site: CAGTGACAAAGTGCTTAAGT), and synthesized oligos for knockin (50mer arm+1bp+50mer arm: CAGTCAAGAAAAATAAGAGACACATGGCTGAGGTGAATGCATCCCCACT-t/c-TAAGCACTTTGTCACTGCCAAGAAGAAGATCAATGGCATTTTTGAGCAGC), the electroporator NEPA21 (NEPAGENE) was used for introducing plasmid DNAs into hiPS cells as described (*Sato et al., 2019*). Cultured hiPS cells transfected with pX458-*hMFN2* were dissociated with TrypLE select (GIBCO) at 37°C for 5 min for detecting transfected cells. Dissociated cells were resuspended with 1% bovine serum albumin in PBS. Cell debris was eliminated with a cell strainer (35μm), and dissociated cell suspensions were centrifuged and stained with SYTOX Red Dead Cell Stain (Molecular Probes) to exclude dead cells. Single GFP-positive cells on the 96-well cell culture plate were collected by FACSJAZZ. Sorted single cells were expanded for a few weeks to analyze genomic DNA.

3D-Clinostat

3D-Clinostat (Zeromo CL-5000, Kitagawa Corporation) was used to produce microgravity conditions by rotating a sample around two axes, creating a pseudo-environment similar to that of outer space (1/1000 G), Differentiated human myotubes or human iPS cells were cultured in cell culture dishes (35mm, Corning) for 48 hours or 7 days in simulated microgravity. while cells in the same dishes were cultured under 1G ground conditions as a control. The use of a gravity acceleration sensor helped to define the simulated microgravity conditions within a few minutes. A detailed description of the metabolic analyses with myogenic cells cultured in microgravity conditions will be published elsewhere (Sugiura et al., in preparation).

RNA-seq Analysis

Total RNAs from cultured human iPS cells were extracted using NucleoSpin RNA Plus XS (Macherey-Nagel). The 100 ng of total RNAs were used as starting materials to generate RNA-seq libraries with the TruSeq Stranded mRNA LT sample prep kit (Illumina). The obtained libraries were sequenced on a NextSeq500 (Illumina) as 75 bp single-end reads. After trimming adaptor sequences and low-quality bases with cutadapt-1.18, the sequenced reads were mapped to the mouse reference genome (mm10) with STAR v 2.6.0c, with the GENCODE (release 36, GRCh38.p13) gtf file. The raw counts for each gene were calculated using htseq-count v0.11.2 with the GENCODE

gtf file. Gene expression levels were determined as transcripts per million (TPM) and differentially expressed genes were identified with DESeq2 v1.30.1. Raw data concerning this study were submitted under Gene Expression Omnibus (GEO) accession number GSE226330.

RT-qPCR analyses

Total RNAs from sorted or cultured cells were extracted using NucleoSpin RNA Plus XS. For quantitative PCR analyses, synthesized cDNAs were prepared using SuperScript VILO MasterMix (Invitrogen). All RT-qPCR reactions were carried out in triplicate using ThunderBird SYBR qPCR Mix (TOYOBO) and Thermal Cycler Dice Realtime System (TAKARA), and normalized to mRNA expression level of human *ribosomal protein L13A, GAPDH, and ACTB* as controls. Primer sequences (5' to 3') are listed in *Supplementary file 16*.

Western Blot

The cells were lysed with radio-immunoprecipitation assay (RIPA) buffer (Nacalai tesque) or ProteoExtract Subcellular Proteome Extraction Kit (Millipore) containing a protease inhibitor cocktail (Nacalai tesque). The supernatant containing the total proteins was fractionated after centrifugation by sodium dodecyl sulfate (SDS)-polyacrylamide gel electrophoresis (TEFCO). The separated proteins were transferred to polyvinylidene difluoride membranes (TEFCO), blocked with 5% of BlockingOne (Nacalai tesque) for 30 minutes, and incubated with anti-MFN2 (diluted 1/1000, Cell Signaling Technology), anti-MuRF1 (diluted 1/2000, GeneTex), anti-FBXO32 (diluted 1/2000, Proteintech), anti-NICD (diluted 1/1000, Cell Signaling Technology), anti-AKT (pan, diluted 1/1000, Cell Signaling Technology), anti-Phospho-AKT (Ser473, diluted 1/2000, Cell Signaling Technology), anti-Histon H3 (diluted 1/1000, Abcam), anti-Hsp601 (HSPD1, diluted 1/1000, Abcam), and anti-GAPDH (diluted 1/1000, Abcam) primary antibodies overnight at 4 °C. The blots were probed with horseradish peroxidase-conjugated secondary antibodies (Molecular Probes; diluted 1/5000) and developed with luminal for enhanced chemiluminescence using Chemi-Lumi One Super (Nacalai tesque). When probing for multiple targets, a single membrane was stripped with WB Stripping Solution (Nacalai tesque) and re-probed with antibodies again.

Immunofluorescence

Cultured cells were fixed with 4% paraformaldehyde in PBS for 15 minutes at 4°C. Subsequently, the samples were incubated with 0.1% TritonX-100 in PBS for 5 minutes and then blocked with BlockingOne for 30 minutes. The cells were then incubated overnight at 4°C with a variety of primary antibodies including anti-MFN2 (Cell Signaling Technology; diluted 1:200), anti-TRA-1-81 (diluted 1:200, Cell Signaling Technology), anti-NANOG (diluted 1:200, Cell Signaling Technology), anti-NICD (diluted 1/200, Abcam), anti-NOTCH2 ICD (N2ICD, dilute 1/200, R&D), anti-PAX7 (diluted 1/100, DSHB), anti-Myogenin (diluted 1/100, DAKO), anti-MYH3 (diluted 1/100, DSHB), anti-Laminin 2a (diluted 1/500, Enzo Life Sciences), anti-Dystrophin (diluted 1/200, Abcam), anti-Caspase3 (diluted 1/100, Proteintech) antibodies in 5% of BlockingOne in PBS with 0.1% Tween20 (PBST). Following three washes with PBST, the cells were incubated with Alexa-conjugated anti-mouse, rabbit, or rat IgG antibodies (Molecular Probes; diluted 1/500). The cells were then washed and mounted in ProLong Diamond antifade reagent with DAPI (Molecular Probes) and images were collected and processed using a BZX-700 microscopy (Keyence).

Visualized MAMs with Proximity ligation assay (PLA)

Fixed cells with 4%PFA solution washed with PBS and blocked with BlockingOne for 30 minutes at room temperature. Next, anti-IP3R (diluted 1/200, Abcam) and anti-VDAC1 (diluted 1/200, Abcam) primary antibodies were incubated overnight at 4°C. Following washing with PBS, MAM was visualized using Duolink PLA Reagents (Sigma-Aldrich). Secondary antibodies conjugated with anti-mouse PLUS and anti-rabbit MINUS oligonucleotides were incubated for 1 hour at 37°C. After a 30 minutes reaction at 37°C using Ligation solution mixed with 5× Ligation stock and Ligase, the

sample was incubated with Amplification solution, containing 5× Amp Red solution and polymerase, for 100 minutes at 37°C. MAM signals, visualized as red particles, were quantified using a hybrid cell counting system (Keyence).

Enzymatic activity assay

The intracellular ATP levels were determined using the luciferase method with ATP Assay Kit-Luminescence (DOJINDO) as per the manufacturer's instructions. Briefly, collected cells were washed with PBS, and lysed using an attached Assay Buffer. The supernatant was incubated with a freshly prepared Working solution containing substrate and enzyme solution and then subjected to bioluminescent detection using a microplate reader (Infinite 200 PRO, TECAN). The ATP level was measured as a control with 1µmol/l of ATP stock solution. Calcineurin activity was measured using a cellular calcineurin phosphatase activity assay kit (Abcam), following the manufacturer's instruction by the microplate reader.

Mouse lines

All animal experiments were approved by the ethics committee of Animal Experimentation of Fujita Health University (Permission number AP18019). Needle injections were performed under anesthesia, and all efforts were made to minimize suffering. *MFN2*$^{loxP/+}$(Jackson Laboratory #026525), *Pax7*$^{CreERT2/+}$ (Jackson Laboratory #017763) mice were used to obtain skeletal muscle cells, 4-hydroxytamoxifen (4-OHT; Sigma-Aldrich) was administrated to 12 weeks old male mice at a dose of 1.0mg/40g body weight via intraperitoneal injection for five consecutive days. Female *Dmd*$^{-/y}$ mice crossed with male NSG mice (Charles River) (*Sato et al., 2014*) were used as transplanted donors. Male *Dmd*$^{-/y}$; NSG mice were used for all experiments at the indicated ages.

Mouse MuSCs sorting

For the isolation and culture of live skeletal muscle stem cells in mice, *tibialis anterior* (TA) muscles were treated with 0.1% Collagenase Type2 in DMEM/F12 at 37°C for 60 minutes. The dissociated cells were resuspended with 1% BSA in PBS and filtrated through a cell strainer. The cell suspensions were stained with anti-SM-C/2.6 antibody (*Fukada et al., 2004*) as well as anti-CD45-PE (diluted 1/500, Biolegend), anti-CD31-PE (diluted 1/500, Biolegend), anti-Sca1-PE (diluted 1/500, Biolegend) antibodies to exclude non-muscle cells.

Grafting of MuSCs into TA muscles of DMD mice

Dmd$^{-/y}$; NSG host male mice aged 12 weeks were used for engraftment of freshly isolated MuSCs derived from wildtype or conditional Mfn2 knockout mice ($1.0x10^4$ cells per 20µL of PBS) into TA muscles. TA muscle was removed 2 weeks after transplantation with several injections of DAPT solution (20µL of 50µM stock, WAKO) as shown in **Fig. 5E**, fixed, and stained as above. For quantification, serial transverse sections were cut across the entire TA muscle, generating approximately 20 slides per muscle, each containing about 20 serial sections. Five distinct slides were immunostained, encompassing regions where the majority of engrafted cells were located, to quantify the number of Dystrophin-positive (doner cells) or Lama2-positive (whole) myofibers using a hybrid cell counting system. At least four transplanted mice were analyzed per experiment.

Statistics

We present statistical data, including the results of multiple biological replicates. The statistical analyses were conducted using Prism9 software (GraphPad Software), employing non-parametric Wilcoxon tests to compare two factors, and one-way ANOVA followed by Tukey's comparison test to determine significant differences among more than three factors. The p-values are indicated on each figure and considered significant when <0.05. All error bars are represented as means ± SEM unless otherwise stated.

Acknowledgements

This work was supported by the Japan Society for the Promotion of Science, KAKENHI grants 17K01859, 18H04061, 23K10971, Japan Agency for Medical Research and Development (AMED) CREST 21gm0910009h0506, the Nakatomi Memorial Foundation, and the Hori Sciences and Arts Foundation. The author declared no conflict of interest.

Author contributions

Yurika Ito, Data curation, Formal analysis, Validation, Investigation, Visualization; Mari Yamagata, Data curation, Formal analysis, Validation, Investigation, Visualization; Takuya Yamamoto, Data curation, Software, Formal analysis, Validation; Katsuya Hirasaka, Data curation, Formal analysis, Visualization; Takeshi Nikawa, Conceptualization, Resources, Supervision ; Takahiko Sato, Conceptualization, Supervision, Funding acquisition, Writing - original draft, Project administration, Writing – review and editing

References

Alam MS (2018) **Proximity Ligation Assay (PLA)** *Curr Protoc Immunol* **123** https://doi.org/10.1002/cpim.58

Andersson ER, Sandberg R, Lendahl U (2011) **Notch signaling: simplicity in design, versatility in function** *Development* **138**:3593–612 https://doi.org/10.1242/dev.063610

Balaganapathy P, Baik SH, Mallilankaraman K, Sobey CG, Jo DG, Arumugam TV (2018) **Interplay between Notch and p53 promotes neuronal cell death in ischemic stroke** *J Cereb Blood Flow Metab* **38**:1781–1795 https://doi.org/10.1177/0271678X17715956

Bhattacharya D, Scimè A (2020) **Mitochondrial Function in Muscle Stem Cell Fates** *Front Cell Dev Biol* **8** https://doi.org/10.3389/fcell.2020.00480

Bi P, Yue F, Sato Y, Wirbisky S, Liu W, Shan T, Wen Y, Zhou D, Freeman J, Kuang S (2016) **Stage-specific effects of Notch activation during skeletal myogenesis** *Elife* **5** https://doi.org/10.7554/eLife.17355

Bodine SC *et al.* (2001) **Identification of ubiquitin ligases required for skeletal muscle atrophy** *Science* **294**:1704–1708 https://doi.org/10.1126/science.1065874

Bonfanti A, Duque J, Kabla A, Charras G (2022) **Fracture in living tissues** *Trends Cell Biol* **32**:537–551 https://doi.org/10.1016/j.tcb.2022.01.005

Bröhl D, Vasyutina E, Czajkowski MT, Griger J, Rassek C, Rahn HP, Purfürst B, Wende H, Birchmeier C (2012) **Colonization of the satellite cell niche by skeletal muscle progenitor cells depends on Notch signals** *Dev Cell* **23**:469–481 https://doi.org/10.1016/j.devcel.2012.07.014

Cartoni R, Martinou JC (2009) **Role of mitofusin 2 mutations in the physiopathology of Charcot-Marie-Tooth disease type 2A** *Exp Neurol* **218**:268–73 https://doi.org/10.1016/j.expneurol.2009.05.003

Chen H, Detmer SA, Ewald AJ, Griffin EE, Fraser SE, Chan DC (2003) **Mitofusins Mfn1 and Mfn2 coordinately regulate mitochondrial fusion and are essential for embryonic development** *J. Cell Biol* **160**:189–200 https://doi.org/10.1083/jcb.200211046

Chen H, Vermulst M, Wang YE, Chomyn A, Prolla TA, McCaffery JM, Chan DC (2010) **Mitochondrial Fusion Is Required for mtDNA Stability in Skeletal Muscle and Tolerance of mtDNA Mutations** *Cell* **141**:280–289 https://doi.org/10.1016/j.cell.2010.02.026

Chen Y, Dorn GW (2013) **PINK1-phosphorylated mitofusin 2 is a Parkin receptor for culling damaged mitochondria** *Science* **340**:471–5 https://doi.org/10.1126/science.1231031

de Brito OM, Scorrano L (2008) **Mitofusin 2 tethers endoplasmic reticulum to mitochondria** *Nature* **456**:605–610 https://doi.org/10.1038/nature07534

D'Eletto M *et al.* (2018) **Transglutaminase Type 2 Regulates ER-Mitochondria Contact Sites by Interacting with GRP75** *Cell Rep* **25**:3573–3581 https://doi.org/10.1016/j.celrep.2018.11.094

Delfini MC, Hirsinger E, Pourquié O, Duprez D (2000) **Delta1-activated notch inhibits muscle differentiation without affecting Myf5 and Pax3 expression in chick limb myogenesis** *Development* **127**:5213–5224 https://doi.org/10.1242/dev.127.23.5213

Distefano G, Goodpaster BH (2018) **Effects of Exercise and Aging on Skeletal Muscle** *Cold Spring Harb Perspect Med* **8** https://doi.org/10.1101/cshperspect.a029785

Duguez S, Féasson L, Denis C, Freyssenet D (2002) **Mitochondrial biogenesis during skeletal muscle regeneration** *Am J Physiol Endocrinol Metab* **282**:E802–9 https://doi.org/10.1152/ajpendo.00343.2001

Eura Y, Ishihara N, Yokota S, Mihara K (2003) **Two mitofusin proteins, mammalian homologues of FZO, with distinct functions are both required for mitochondrial fusion** *J Biochem* **134**:333–344 https://doi.org/10.1093/jb/mvg150

Ferrari-Toninelli G, Bonini SA, Uberti D, Buizza L, Bettinsoli P, Poliani PL, Facchetti F, Memo M (2010) **Targeting Notch pathway induces growth inhibition and differentiation of neuroblastoma cells** *Neuro Oncol* **12**:1231–43 https://doi.org/10.1093/neuonc/noq101

Filadi R, Pendin D, Pizzo P (2018) **Mitofusin 2: from functions to disease** *Cell Death Dis* **9** https://doi.org/10.1038/s41419-017-0023-6

Fujimaki S *et al.* (2022) **The endothelial Dll4-muscular Notch2 axis regulates skeletal muscle mass** *Nat. Metab* **4**:180–189 https://doi.org/10.1038/s42255-022-00560-6

Fukada S *et al.* (2004) **Purification and cell-surface marker characterization of quiescent satellite cells from murine skeletal muscle by a novel monoclonal antibody** *Exp Cell Res* **296**:245–55 https://doi.org/10.1016/j.yexcr.2004.02.018

Gao Y, Arfat Y, Wang H, Goswami N (2018) **Muscle Atrophy Induced by Mechanical Unloading: Mechanisms and Potential Countermeasures** *Front. Physiol* **9** https://doi.org/10.3389/fphys.2018.00235

Gioftsidi S, Relaix F, Mourikis P (2022) **The Notch signaling network in muscle stem cells during development, homeostasis, and disease** *Skelet. Muscle* **12** https://doi.org/10.1186/s13395-022-00293-w

Gottschalk B, Koshenov Z, Bachkoenig OA, Rost R, Malli R, Graier WF (2022) **MFN2 mediates ER-mitochondrial coupling during ER stress through specialized stable contact sites** *Front Cell Dev Biol* **10** https://doi.org/10.3389/fcell.2022.918691

Hardy D *et al.* (2016) **Comparative study of injury models for studying muscle regeneration in mice** *PLoS One* **11** https://doi.org/10.1371/journal.pone.0147198

Ishihara N, Eura Y, Mihara K (2004) **Mitofusin 1 and 2 play distinct roles in mitochondrial fusion reactions via GTPase activity** *J. Cell Sci* **117**:6535–46 https://doi.org/10.1242/jcs.01565

Kasahara A, Cipolat S, Chen Y, Dorn GW, Scorrano L (2013) **Mitochondrial fusion directs cardiomyocyte differentiation via calcineurin and Notch signaling** *Science* **342**:734–737 https://doi.org/10.1126/science.1241359

Larsson L, Degens H, Li M, Salviati L, Lee YI, Thompson W, Kirkland JL, Sandri M (2019) **Sarcopenia: Aging-Related Loss of Muscle Mass and Function** *Physiol Rev* **99**:427–511 https://doi.org/10.1152/physrev.00061.2017

Lim D, Dematteis G, Tapella L, Genazzani AA, Calì T, Brini M, Verkhratsky A (2021) **Ca2+ handling at the mitochondria-ER contact sites in neurodegeneration** *Cell Calcium* **98** https://doi.org/10.1016/j.ceca.2021.102453

Liu L, Charville GW, Cheung TH, Yoo B, Santos PJ, Schroeder M, Rando TA (2018) **Impaired Notch Signaling Leads to a Decrease in p53 Activity and Mitotic Catastrophe in Aged Muscle Stem Cells** *Cell Stem Cell* **23**:544–556 https://doi.org/10.1016/j.stem.2018.08.019

Ljubicic V, Joseph AM, Saleem A, Uguccioni G, Collu-Marchese M, Lai RYJ, Linda M-D, Nguyen LMD, Hood DA (2010) **Transcriptional and post-transcriptional regulation of mitochondrial biogenesis in skeletal muscle: effects of exercise and aging** *Biochim Biophys Acta* **1800**:223–34 https://doi.org/10.1016/j.bbagen.2009.07.031

Luo N, Yue F, Jia Z, Chen J, Deng Q, Zhao Y, Kuang S (2021) **Reduced electron transport chain complex I protein abundance and function in Mfn2-deficient myogenic progenitors lead to oxidative stress and mitochondria swelling** *FASEB J* **35** https://doi.org/10.1096/fj.202002464R

Mansour J, Berwanger C, Jung M, Eichinger L, Fabry B, Clemen SC (2023) **Clinorotation inhibits myotube formation by fluid motion, not by simulated microgravity** *Eur J Cell Biol* **102** https://doi.org/10.1016/j.ejcb.2023.151330

McCaw TR, Inga E, Chen H, Jaskula-Sztul R, Dudeja V, Bibb JA, Ren B, Rose JB (2021) **Gamma Secretase Inhibitors in Cancer: A Current Perspective on Clinical Performance** *Oncologist* **26**:e608–e621 https://doi.org/10.1002/onco.13627

Ohara R, Imamura K, Morii F, Egawa N, Tsukita K, Enami T, Shibukawa R, Mizuno T, Nakagawa M, Inoue H (2017) **Modeling Drug-Induced Neuropathy Using Human iPSCs for Predictive Toxicology** *Clin Pharmacol Ther* **101**:754–762 https://doi.org/10.1002/cpt.562

Prole DL, Taylor CW (2019) **Structure and Function of IP3 Receptors** *Cold Spring Harb Perspect Biol* **11** https://doi.org/10.1101/cshperspect.a035063

Rand MD, Grimm LM, Artavanis-Tsakonas S, Patriub V, Blacklow SC, Sklar J, Aster JC (2000) **Calcium depletion dissociates and activates heterodimeric notch receptors** *Mol. Cell. Biol* **20**:1825–1835 https://doi.org/10.1128/MCB.20.5.1825-1835.2000

Rizzuto R, Pinton P, Carrington W, Fay FS, Fogarty KE, Lifshitz LM, Tuft RA, Pozzan T (1998) **Close contacts with the endoplasmic reticulum as determinants of mitochondrial Ca2+ responses** *Science* **280**:1763–1766 https://doi.org/10.1126/science.280.5370.1763

Roti G *et al.* (2013) **Complementary genomic screens identify SERCA as a therapeutic target in NOTCH1 mutated cancer** *Cancer Cell* **23**:390–405 https://doi.org/10.1016/j.ccr.2013.01.015

Ryall JG (2013) **Metabolic reprogramming as a novel regulator of skeletal muscle development and regeneration** *FEBS J* **280**:4004–13 https://doi.org/10.1111/febs.12189

Sakai-Takemura F, Nogami K, Elhussieny A, Kawabata K, Maruyama Y, Hashimoto N, Takeda S, Miyagoe-Suzuki Y (2020) **Prostaglandin EP2 receptor downstream of Notch signaling inhibits differentiation of human skeletal muscle progenitors in differentiation conditions. Commun** *Biol* **3** https://doi.org/10.1038/s42003-020-0904-6

Sandri M, Sandri C, Gilbert A, Skurk C, Calabria E, Picard A, Walsh K, Schiaffino S, Lecker SH, Goldberg AL (2004) **Foxo transcription factors induce the atrophy-related ubiquitin ligase atrogin-1 and cause skeletal muscle atrophy** *Cell* **117**:399–412 https://doi.org/10.1016/s0092-8674(04)00400-3

Sato T, Yamamoto T, Sehara-Fujisawa A (2014) **miR-195/497 induce postnatal quiescence of skeletal muscle stem cells** *Nat Commun* **5** https://doi.org/10.1038/ncomms5597

Sato T, Higashioka K, Sakurai H, Yamamoto T, Goshima N, Ueno M, Sotozono C (2019) **Core Transcription Factors Promote Induction of PAX3-Positive Skeletal Muscle Stem Cells** *Stem Cell Reports* **13**:352–365 https://doi.org/10.1016/j.stemcr.2019.06.006

Sebastián D *et al.* (2016) **Mfn2 deficiency links age-related sarcopenia and impaired autophagy to activation of an adaptive mitophagy pathway** *EMBO J* **35**:1677–1693 https://doi.org/10.15252/embj.201593084

Shoshan-Barmatz V, Hadad N, Feng W, Shafir I, Orr I, Varsanyi M, Heilmeyer LM (1996) **VDAC/porin is present in sarcoplasmic reticulum from skeletal muscle** *FEBS Lett* **386**:205–10 https://doi.org/10.1016/0014-5793(96)00442-5

Sin J, Andres AM, Taylor DJR, Weston T, Hiraumi Y, Stotland A, Kim BJ, Huang C, Doran KS, Gottlieb RA (2016) **Mitophagy is required for mitochondrial biogenesis and myogenic differentiation of C2C12 myoblasts** *Autophagy* **12**:369–380 https://doi.org/10.1080/15548627.2015.1115172

Song Z, Song H, Liu D, Yan B, Wang D, Zhang Y, Zhao X, Tian X, Yan C, Han Y (2022) **Overexpression of MFN2 alleviates sorafenib-induced cardiomyocyte necroptosis via the MAM-CaMKIIδ pathway in vitro and in vivo** *Theranostics* **12**:1267–1285 https://doi.org/10.7150/thno.65716

Szabadkai G, Bianchi K, Várnai P, De Stefani D, Wieckowski MR, Cavagna D, Nagy AI, Balla T, Rizzuto R (2006) **Chaperone-mediated coupling of endoplasmic reticulum and mitochondrial Ca2+ channels** *J. Cell Biol* **175**:901–911 https://doi.org/10.1083/jcb.200608073

Takahashi K, Tanabe K, Ohnuki M, Narita M, Ichisaka T, Tomoda K, Yamanaka S (2007) **Induction of pluripotent stem cells from adult human fibroblasts by defined factors** *Cell* **131**:861–72 https://doi.org/10.1016/j.cell.2007.11.019

Tanaka A *et al.* (2013) **Efficient and reproducible myogenic differentiation from human iPS cells: prospects for modeling Miyoshi Myopathy in vitro** *PLoS One* **8** https://doi.org/10.1371/journal.pone.0061540

Theurey P, Tubbs E, Vial G, Jacquemetton J, Bendridi N, Chauvin MA, Alam MR, Le Romancer M, Vidal H, Rieusset J (2016) **Mitochondria-associated endoplasmic reticulum membranes allow adaptation of mitochondrial metabolism to glucose availability in the liver** *J. Mol. Cell Biol* **8**:129–43 https://doi.org/10.1093/jmcb/mjw004

Valon L, Levayer R (2019) **Dying under pressure: cellular characterisation and in vivo functions of cell death induced by compaction** *Biol Cell* **111**:51–66 https://doi.org/10.1111/boc.201800075

Wyckelsma VL, Levinger I, McKenna MJ, Formosa LE, Ryan MT, Petersen AC, Anderson MJ, Murphy RM (2017) **Preservation of skeletal muscle mitochondrial content in older adults: relationship between mitochondria, fibre type and high-intensity exercise training** *J. Physiol* **595**:3345–3359 https://doi.org/10.1113/JP273950

Yamanaka Y, Takenaka N, Sakurai H, Ueno M, Kinoshita S, Sotozono C, Sato T (2019) **Human Skeletal Muscle Cells Derived from the Orbicularis Oculi Have Regenerative Capacity for Duchenne Muscular Dystrophy** *Int. J. Mol. Sci* **20** https://doi.org/10.3390/ijms20143456

You WK, Schuetz TJ, Lee SH (2023) **Targeting the DLL/Notch Signaling Pathway in Cancer: Challenges and Advances in Clinical Development** *Mol Cancer Ther* **22**:3–11 https://doi.org/10.1158/1535-7163.MCT-22-0243

Youle RJ, van der Bliek AM (2012) **Mitochondrial Fission, Fusion, and Stress** *Science* **337**:1067–5 https://doi.org/10.1126/science.1219855

Article and author information

Yurika Ito
Faculty of Medical Sciences, Fujita Health University, Toyoake, Japan

Mari Yamagata
Department of Biomedical Engineering, Faculty of Life and Medical Sciences, Doshisha University, Kyotanabe, Japan

Takuya Yamamoto
Center for iPS Cell Research and Application, Kyoto University, Kyoto, Japan
ORCID iD: 0000-0002-0022-3947

Katsuya Hirasaka
Organization for Marine Science and Technology, Nagasaki University Graduate School, Nagasaki, Japan
ORCID iD: 0000-0003-2645-8450

Takeshi Nikawa
Department of Nutritional Physiology, Institute of Medical Nutrition, Tokushima University Graduate School, 3-18-15 Kuramoto-cho, Tokushima, Japan

Takahiko Sato
Department of Ophthalmology, Kyoto Prefectural University of Medicine, Kyoto, Japan,
Department of Anatomy, Faculty of Medicine, Fujita Health University, Toyoake, Japan,
International Center for Cell and Gene Therapy, Fujita Health University, Toyoake, Japan
For correspondence: takahiko@fujita-hu.ac.jp
ORCID iD: 0000-0003-3836-7978

Copyright

source are credited.

Editors

Reviewing Editor
Graziana Colaianni
University of Bari, Italy

Senior Editor
Carlos Isales
Augusta University, United States of America

Reviewer #1 (Public Review):

In this study, the authors investigated the role of MAM and the Notch signalling pathway in the onset of the atrophic phenotype in both in vivo and in vitro models. The rationale used to obtain the data is one of the main strengths of the study. Already from the reading, the reasoning scheme used by the authors in setting up the study and evaluating the data obtained is clear. Using both cellular and mouse models in vivo consolidates the data obtained. The authors also methodologically described all the choices made in the supplementary section.

Reviewer #2 (Public Review):

In this study, the authors examined how maintenance of mitochondrial-associated endoplasmic reticulum membranes (MAM) are critical for the prevention of muscle atrophy under microgravity conditions. They observed, a reduction in MAM in myotubes placed in a microgravity condition; in addition, MFN2-deficient human iPS cells showed a decrease in the number of MAM, similar to in myotubes differentiated under microgravity conditions, in addition to the activation of the Notch signaling pathway. The authors, morover, obsreved that by treatment with the gamma-secretase inhibitor with DAPT preserved from the atrophic phenotype of differentiated myotubes in microgravity and improve the regenerative capacity of Mfn2-deficient muscle stem cells in dystrophic mice.

The entire study was well conducted, bringing an interesting analysis in vitro and in vivo of aging condition. In my opinion it is necessary to implement the analysis of both genes and proteins for better supporting the conclusions

The study can contribute to better understand one of the major problems of aging, such as muscle atrophy and inhibition of muscle regeneration, emphasizing the importance of NOTCH patway in these pathological situations. The work will be of interest to all scientist working on aging.

Author Response

The following is the authors' response to the original reviews.

> ***Reviewer #1 (Public Review):***
>
> *In this study, the authors investigated the role of MAM and the Notch signaling pathway in the onset of the atrophic phenotype in both in vivo and in vitro models. The rationale used to obtain the data is one of the main strengths of the study. Already from the reading, the reasoning scheme used by the authors in setting up the study and evaluating the data obtained is clear. Using both cellular and mouse models in vivo consolidates the data obtained. The authors also methodologically described all the choices made in the supplementary section. A weakness, on the other hand, is the failure*

> *to include averages and statistical data in the results that would give a quantifiable idea of the data obtained. To complete the picture, the authors could also investigate the possible involvement of the intrinsic apoptosis pathway as well as describe probable metabolic shifts to muscle cells in atrophic conditions. The rationale used by the authors to obtain the result is linear. The data obtained are useful for understanding the onset and characterization of the atrophic phenotype under disuse and microgravity conditions. The methods used are in line with those used in the field and can be a starting point for other studies. The cellular models are well described in the Materials and methods section. The selected mouse models followed a logical rationale and were in line with the intended aim.*

We thank this reviewer for comments that have led us to clarify several points.

> ***Reviewer #1 (Recommendations For The Authors):***
>
> - *In order to reinforce and justify the results obtained, I would suggest that the authors include numerical and statistical data in the results obtained.*

Answer) As the reviewer suggested, we have incorporated actual numerical and statistical data into each graph in all figures.

> - *With the aim of better framing the picture of an atrophic muscle phenotype caused by microgravity or disuse, I would advise the authors to also focus on the possible involvement of the intrinsic apoptosis pathway. To this end, it would be interesting to assess a possible relationship between MAM and apoptosis. It would be useful to integrate this part into the discussion.*

Answer) It has been shown that suppression of Mfn2 expression attenuates calcium influx into mitochondria during apoptosis-inducing stimuli, thereby inhibiting apoptosis (Martins de Brito & Scorrano, Nature 2008), however, in our study, we found that apoptotic pathways, including Caspase3 or p-AKT were not significantly altered in differentiated human myocytes by microgravity for 7 days in culture, suggesting that microgravity-induced apoptosis is not an initial pathway to MAM. We have added these data in the new supplementary file 3 and mentioned it in the results.

> - *In addition to TA, did the authors investigate what was seen in other muscles impacted by microgravity? If so, I would recommend supplementing what is available or, on the contrary, justifying the exclusivity of the choice of TA.*

Answer) It has been reported that the soleus, a slow-type muscle is more susceptible than the fast-type tibialis anterior muscle during gravity changes, so it makes more sense for the content of this study to analyze the soleus muscle. However, we chose the tibialis anterior muscle as our target because it provides the most stable results as a site for stem cell transplantation to observe muscle regeneration.

> - *The authors affirm that there is an altered distribution and morphology of mitochondria under microgravity conditions. To corroborate this assertion, I would recommend including a morphological image that confirms it.*

Answer) The morphology of mitochondria in cultured myotubes, as observed by mitotracker staining in Figure 4G, varied widely, from finely divided to fused even within a single fiber compared to MFN2-mutated human iPS cells, making it difficult to conclude whether these changes were brought about by microgravity. Therefore, in this study, we have shown that

they are reduced in microgravity by the difference in fluorescence intensity of mitotracker, which is directly proportional to mitochondrial activity.

> - *It would be interesting if the authors would show whether there are changes in myosin expression or metabolic changes in cells subjected to microgravity and in the cell model with Mnf2 deletion. It would also be interesting to evaluate this in the presence of DAPT.*

Answer) As the reviewer's suggestion, we have checked MYH1, MYH3, and MYH7 transcripts in differentiated myotubes under microgravity, with or without DAPT in the new supplementary file 12. We have added the data showing that not MYH1 but MYH7 transcript was partially recovered in the Results.

A detailed description of the metabolic analyses with myogenic cells cultured in microgravity conditions will be published elsewhere (Sugiura et al., "Mitochondria aconitase is a main target for unloading-mediated mitochondria dysfunction toward muscle atrophy", in preparation). We have described it in the Materials and methods of the manuscript.

> ***Reviewer #2 (Public Review):***
>
> *In this study, the authors examined how the maintenance of mitochondrial-associated endoplasmic reticulum membranes (MAM) is critical for the prevention of muscle atrophy under microgravity conditions. They observed, a reduction in MAM in myotubes placed in a microgravity condition; in addition, MFN2-deficient human iPS cells showed a decrease in the number of MAM, similar to in myotubes differentiated under microgravity conditions, in addition to the activation of the Notch signaling pathway. The authors, moreover, observed that treatment with the gamma-secretase inhibitor with DAPT preserved the atrophic phenotype of differentiated myotubes in microgravity and improve the regenerative capacity of Mfn2-deficient muscle stem cells in dystrophic mice. The entire study was well conducted, bringing an interesting analysis in vitro and in vivo of aging conditions. In my opinion, it is necessary to improve the analysis of both genes and proteins to better support the conclusions*
>
> *The study can contribute to a better understanding of one of the major problems of aging, such as muscle atrophy and inhibition of muscle regeneration, emphasizing the importance of the NOTCH pathway in these pathological situations. The work will be of interest to all scientists working on aging*

We thank this reviewer for the positive comments and remarks that we have attempted to address.

> ***Reviewer #2 (Recommendations For The Authors):***
>
> *Results:*
>
> *In Figure 1b authors observed an increase in the transcripts of MuRF1 and FBXO32 after 7 days of microgravity condition. I suggest to investigate the protein expression of these genes to give more validation to this data.*

Answer) As the reviewer's suggestion, we have investigated the western blotting with atrophic markers in microgravity samples. These data have been added in Figure 1D.

> *Moreover, I suggest investigating not only Myogenin as an earlier gene of myotubes formation but also MRF4.*
>
> *Methods:*

> *I suggest when doing real-time PCR not to use a single gene as housekeeping but the average of three genes, to avoid the influence of a single housekeeping gene affecting the results.*

Answer) As the reviewer's suggestion, we have investigated MRF4 expression by qPCR experiments with 3 different housekeeping genes (RPL13a, GAPDH, and ACTB). Our experiments showed no significant differences among these three housekeeping genes. We have added these data to Figure 1C and Methods in the manuscript.